Langtaosha (LTS) Preprint doi: https://doi.org/10.65215/LTSpreprints.2026.11.20.000396. This version posted November 21, 2026. The copyright holder for this preprint (which was not certified by peer review) is the author/funder. All Rights Reserved. No reuse allowed without permission.

In situ reconstruction of the skeletal muscle excitation-contraction coupling ultracomplex

Jiashu Xu[1,3], Jiaao Li[1,3], and Nieng Yan[1,2,4]

[1]Beijing Frontier Research Center for Biological Structure, State Key Laboratory of Membrane Biology, Tsinghua-Peking Joint Center for Life Sciences, School of Life Sciences, Tsinghua University, Beijing 100084, China

[2]Institute of Bio-Architecture and Bio-Interactions (IBABI), Shenzhen Medical Academy of Research and Translation, Guangming District, Shenzhen 518107, Guangdong Province, China

[3]These authors contribute equally to this work.

[4]To whom correspondence should be addressed: N. Yan (nyan@tsinghua.edu.cn).

Langtaosha (LTS) Preprint doi: https://doi.org/10.65215/LTSpreprints.2026.11.20.000396. This version posted November 21, 2026. The copyright holder for this preprint (which was not certified by peer review) is the author/funder. All Rights Reserved. No reuse allowed without permission.

Abstract

Skeletal muscle contraction is governed by excitation-contraction coupling (ECC), a process achieved through the formation of an ultracomplex comprising the $Ca_V1.1$ channel complex on the plasma membrane, the RyR1 complex on the sarcoplasmic reticulum membrane, and several protein components in between. Here we report the *in situ* structures of RyR1 at 4.8-7 Å resolution and of the ECC ultracomplex at an overall resolution of ~ 7 Å, obtained by cryo-electron tomography analysis of focused-ion beam-milled muscle fibers. Calmodulin and FKBP12 are clearly resolved to bind to RyR1. The reconstruction enables identification of the bridging components, including β1a, Junctophilin, and STAC3; their respective interfaces with $Ca_V1.1$ and RyR1 are revealed. The *in situ* analysis of the ultracomplex establishes the foundation for elucidating the molecular basis of ECC.

Langtaosha (LTS) Preprint doi: https://doi.org/10.65215/LTSpreprints.2026.11.20.000396. This version posted November 21, 2026. The copyright holder for this preprint (which was not certified by peer review) is the author/funder. All Rights Reserved. No reuse allowed without permission.

Excitation-contraction coupling (ECC) is the essential physiological process that transduces electrical signals at the plasma membrane (PM) into intracellular chemical and mechanical signaling, centered on calcium release from the sarcoplasmic reticulum (SR). ECC is mediated primarily by two Ca^{2+} channels: the L-type voltage-gated Ca^{2+} (Ca_v) channel (LTCC), also known as the dihydropyridine receptor (DHPR), at the PM and the ryanodine receptor (RyR), the largest ion channel known, at the SR membrane. In skeletal muscle, the plasma membrane invaginates to form a specialized structure called the transverse tubule (T-tubule, TT), which is flanked by terminal cisternae of the SR. $Ca_v1.1$ resides in the TT membrane, whereas RyR1 is the high-conductance Ca^{2+} release channel embedded in the junctional SR membrane [1-3].

$Ca_v1.1$ is a multi-subunit complex composed of the core voltage-sensing and pore-forming subunit α1 and auxiliary subunits, including the extracellular α2δ-1, the transmembrane γ, and the intracellular β1a [4,5]. RyR1 is a homotetramer, with each protomer containing over 5000 residues [6-8]. Blocking Ca^{2+} conductance of $Ca_v1.1$ upon membrane depolarization does not abolish its ability to activate the downstream RyR1, supporting a mechanical coupling mechanism in which signal transduction is achieved by direct transmission of conformational changes from $Ca_v1.1$ to RyR1 [9,10]. In this sense, $Ca_v1.1$ serves as the voltage sensor for RyR1. Their physical association is bridged by additional components. Co-expression of β1a, junctophilin-2 (JP2), and STAC3 with $Ca_v1.1$ and RyR1 can recapitulate their conformational and functional coupling in tsA201 cells [11].

β1a, with a molecular weight of ~ 56 kDa, comprises a guanylate kinase (GK)-like domain and a Src homology three (SH3) domain [12]. As an intrinsic auxiliary subunit of the

Langtaosha (LTS) Preprint doi: https://doi.org/10.65215/LTSpreprints.2026.11.20.000396. This version posted November 21, 2026. The copyright holder for this preprint (which was not certified by peer review) is the author/funder. All Rights Reserved. No reuse allowed without permission.

$Ca_v1.1$ channel complex, its GK domain is associated with the α1-interaction domain (AID) motif, which is an extended helix of the S6 segment in the first repeat ($S6_I$) of $Ca_v1.1α1$ [12]. On the other side, the C-terminal segment of β1a was suggested to directly contact RyR1, possibly with residues 3495-3502 (residue numbering of rabbit RyR1) [13,14].

Junctophilins (JPs) are a family of proteins that help organize the junction structures by bridging the ~ 12-nm gap between the PM and SR membranes [15,16]. Whereas the cytosolic N-terminal region of JPs contains lipid-binding membrane occupation and recognition nexus (MORN) motifs that may interact with the PM, the single C-terminal transmembrane segment is anchored to the SR membrane [15,17]. Expressed in skeletal muscle, JP1 and JP2 are both reported to interact with $Ca_v1.1$, and biochemical evidence for an association with RyR1 is established for JP1 [18,19]. The interaction between JP2 and a C-terminal fragment of $Ca_v1.1α1$ is confirmed by high-resolution crystal structures [20]; the JP contact site on RyR1 remains to be defined.

STAC3, with the full name Src homology three and Cys-rich domain 3, modulates the trafficking and channel activities of $Ca_v1.1$ and is essential for ECC [21-23]. Two contact sites between STAC3 and $Ca_v1.1$ have been reported. One involves the two SH3 domains of STAC3 and the cytosolic loop between repeats II and III (the II-III loops) of $Ca_v1.1α1$, the other concerns the N-terminus of STAC3 and the C-terminus of the channel [24-26].

Despite decades of research, the structural basis of ECC ultracomplex assembly remains incompletely understood, limiting insight into signal transmission across the TT and SR membranes. Electron microscopy has played a central role in the discovery and structural

Langtaosha (LTS) Preprint doi: https://doi.org/10.65215/LTSpreprints.2026.11.20.000396. This version posted November 21, 2026. The copyright holder for this preprint (which was not certified by peer review) is the author/funder. All Rights Reserved. No reuse allowed without permission.

dissection of ECC. As early as the 1970s, Franzini-Armstrong systematically studied the triad, the junction between the TT and SR, and described in detail the electron-dense structures later termed "feet", which are now known to correspond to the cytoplasmic canopy of RyR1. Using electron microscopy together with freeze-fracture techniques, Franzini-Armstrong and collaborators also discovered the tetrad arrangement of DHPRs on the TT membrane and demonstrated that these tetrads correspond to every other RyR1 foot structure on the SR membrane. This "tetrad-foot" spatial matching relationship provided critical insight into how voltage-sensing DHPRs activate the Ca^{2+}-release channel RyR1. [3].

RyR1 has been a prototypical membrane protein for cryo-electron microscopy (cryo-EM) structural studies [27]. Near atomic resolution structures of rabbit RyR1 and $Ca_V1.1$, both isolated from skeletal muscle, were determined soon after the resolution revolution of single-particle cryo-EM [28-31]. Each RyR1 protomer contains the following domains: the amino-terminal domain (NTD), SPRY1, P1, SPRY2, SPRY3, Handle, HD1, P2, HD2, Central domain, the voltage-gated ion channel (VGIC) fold transmembrane domain, and the carboxy terminal domain (CTD) [28]. To date, however, the ECC ultracomplex has not been recapitulated using purified components.

Cryo-electron tomography (cryo-ET), combined with focused ion beam (FIB) milling, has emerged as a powerful tool for visualizing large macromolecular assemblies in their native context [32,33]. A cryo-ET reconstruction of RyR1 within intact mouse muscle cells was obtained at 16.7 Å resolution, and a preliminary map of the ECC ultracomplex was determined at 3-5 nm resolution [34]. This subtomogram averaging (STA) analysis confirmed the "tetrad-foot" assembly

Langtaosha (LTS) Preprint doi: https://doi.org/10.65215/LTSpreprints.2026.11.20.000396. This version posted November 21, 2026. The copyright holder for this preprint (which was not certified by peer review) is the author/funder. All Rights Reserved. No reuse allowed without permission.

and revealed a checkerboard arrangement of the RyR1 arrays. However, the density between the TT and SR membranes was insufficient to support assignment of the bridging proteins.

After we reported the single-particle cryo-EM structures of various Ca_V channels and RyR1 and RyR2 [5,28,35-38], we set out to determine the in situ structure of the ECC ultracomplex using cryo-ET of FIB-milled muscle fibers. Muscle fibers were isolated following a reported protocol, with modifications [39]. Briefly, small chunks of fresh muscle samples were digested with collagenase at 37 °C for 15-20 min, and the resulting muscle fibers were isolated and placed on Quantifoil copper grids for subsequent plunge freezing. The frozen samples were then FIB-milled to prepare lamella with thickness between 100 and 200 nm for cryo-ET imaging (Fig. 1A). Triads, where ECC ultracomplexes are abundant, can be readily targeted manually during data collection (Fig. 1B).

After cumulative data collection over several years, more than 3,200 tilt series were obtained. Over 70,000 RyR1 particles were manually picked for the final STA calculation. During data processing, we found that the *in situ* RyR1 exhibits pronounced dynamics, especially at the peripheral subdomains, such as the helical domains and the P1 and P2 domains; core regions including the NTD, handle, central, and channel domains remain stable. We therefore focused on the core regions for masked image processing. Up to date, an *in situ* 3D reconstruction was obtained at the overall resolution of 4.8-7 Å; the core regions could be resolved to 4.8 Å (Fig. 1C). For visual clarity, different parts of density were contoured at different levels for presentation. As the HD and P2 densities were poor due to high dynamics, we

Langtaosha (LTS) Preprint doi: https://doi.org/10.65215/LTSpreprints.2026.11.20.000396. This version posted November 21, 2026. The copyright holder for this preprint (which was not certified by peer review) is the author/funder. All Rights Reserved. No reuse allowed without permission.

combined densities from another all-RyR1-focused map with an overall resolution of 6 Å for better visualization in this manuscript.

Within the dataset, a set of RyR1 particles with linked densities can be classified and averaged by focusing on RyR1 and linked densities, yielding a 3D reconstruction for the ECC ultracomplex at an overall resolution of 7.1 Å (Fig. 1D). Resolution varies considerably across the complex, with RyR1 best resolved and the transmembrane (TM) region of $Ca_v1.1$ poorest. Fortunately, the characteristic lion-head-shaped density allows unambiguous assignment of the α2δ-1 subunit and, consequently, identification of its tightly associated α1 subunit. Four copies of the $Ca_v1.1$ complex could thus be characterized on top of a tetrameric RyR1 (Fig. 1D).

From the side view, the ECC complex has a height of ~ 38 nm. Importantly, the previously least well-understood bridging components between the TT and SR membranes are well resolved, with the best-resolved part reaching ~ 7 Å (Fig. 1D). The TM region of the tetrad, comprising the voltage-sensing domains (VSDs) of $Ca_v1.1$α1 and the γ subunit that binds to VSD_{IV}, appears as a square in the extracellular view. The square of the $Ca_v1.1$ tetrad TM displays a ~ 35° rotation relative to that of the RyR1 canopy. Viewed from the extracellular side, the two concentric squares adopt a shape resembling the Star of Lakshmi (Fig. 1D).

Of note, calmodulin (CaM) and FK506 binding protein 12 (FKBP12) are clearly resolved in the *in situ* reconstructions of both RyR1 and the ECC ultracomplex (Fig. 1C,D), although CaM is missing in the structures of rabbit RyR1 embedded in isolated native vesicles. The most important finding concerns the resolution of the bridging components between $Ca_v1.1$ and RyR1.

Langtaosha (LTS) Preprint doi: https://doi.org/10.65215/LTSpreprints.2026.11.20.000396. This version posted November 21, 2026. The copyright holder for this preprint (which was not certified by peer review) is the author/funder. All Rights Reserved. No reuse allowed without permission.

The arch-shaped densities that attach to each of the four clamps of RyR1 are reminiscent of the MORN motifs of JP. Their contiguous densities are most likely those of β1a. A narrower strip of density nearly parallel to that of JP may belong to STAC3 (Fig. 1D). The reconstruction of the ECC ultracomplex thus reveals the detailed assembly of β1a, JP, and STAC3, which bridge $Ca_v1.1\alpha1$ and RyR1.

In summary, here we present the *in situ* 3D reconstruction of RyR1 from the skeletal muscle fibers at an averaged resolution of 4.8-7 Å and of the ECC ultracomplex at ~ 7 Å. Our *in situ* analysis provides a framework for understanding the coupling of electromechanical and chemical signals that trigger muscle contraction. Additional data collection and further classification of a larger dataset may yield 3D reconstructions of higher resolution.

Langtaosha (LTS) Preprint doi: https://doi.org/10.65215/LTSpreprints.2026.11.20.000396. This version posted November 21, 2026. The copyright holder for this preprint (which was not certified by peer review) is the author/funder. All Rights Reserved. No reuse allowed without permission.

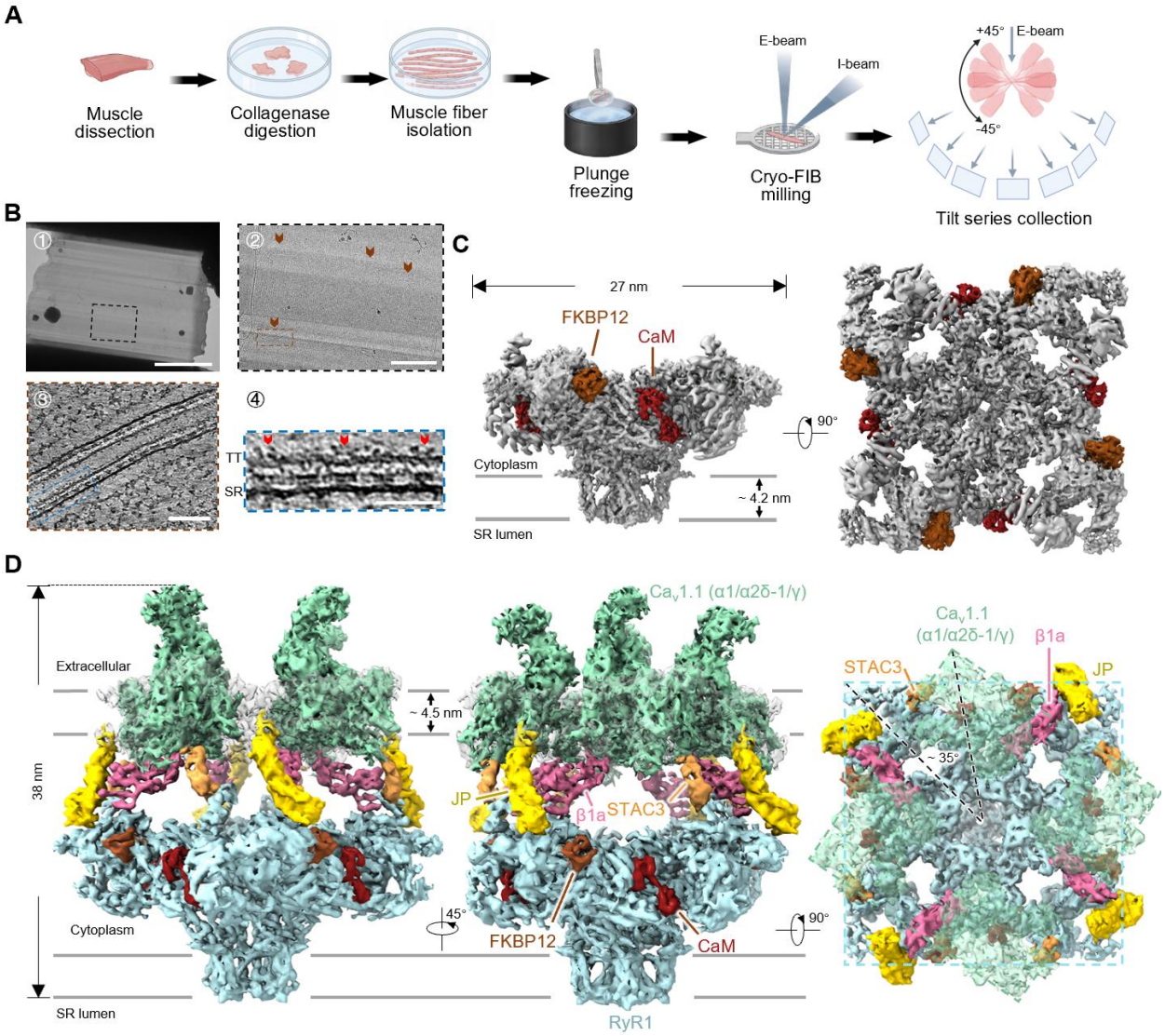


Fig. 1 | Cryo-ET structural determination of the ECC ultracomplex from the FIB-milled muscle fibers. **A**, Schematic workflow of muscle fiber isolation, FIB-milling, and cryo-ET data collection of the ECC ultracomplex. **B**, Data collection and processing. (1) Representative tomogram. Scale bar: 5 μm. (2) Zoomed-in view of the area rich in triads. Brown arrows mark positions of triads. Scale bar: 500 nm. (3) Tomogram of a representative triad. Scale bar: 100 nm. (4) Zoomed-in view of the tomogram rich in ECC complex particles. Red arrows mark the ECC complexes. Scale bar: 50 nm. **C**, An *in situ* reconstruction of RyR1 bound with FKBP12 and CaM. A side and a cytoplasmic view are shown. The resolution is not uniform, decreasing from the center to the periphery. Therefore, the densities were contoured at different levels in accordance with their resolutions for visual clarity. **D**, Overall 3D reconstruction of the ECC complex determined at ~ 7 Å. Three perpendicular views are shown. Each resolved protein component is given a distinct color, except the $Ca_v1.1$ complex, whose extracellular α2δ-1 and transmembrane α1 and γ subunits are all colored green. The same color code for ECC components is applied throughout the manuscript. All EM maps were prepared in ChimeraX.

Langtaosha (LTS) Preprint doi: https://doi.org/10.65215/LTSpreprints.2026.11.20.000396. This version posted November 21, 2026. The copyright holder for this preprint (which was not certified by peer review) is the author/funder. All Rights Reserved. No reuse allowed without permission.

References:

1. Franzini-Armstrong, C. (2024). An updated view of the structural basis for dihydropyridine receptors-ryanodine receptors direct molecular interaction in skeletal muscle. Eur J Transl Myol *34*. 10.4081/ejtm.2024.12476.
2. Bers, D.M. (2002). Cardiac excitation-contraction coupling. Nature *415*, 198-205. 10.1038/415198a.
3. Franzini-Armstrong, C. (2018). The relationship between form and function throughout the history of excitation-contraction coupling. J Gen Physiol *150*, 189-210. 10.1085/jgp.201711889.
4. Huang, J., Pan, X., and Yan, N. (2024). Structural biology and molecular pharmacology of voltage-gated ion channels. Nat Rev Mol Cell Biol *25*, 904-925. 10.1038/s41580-024-00763-7.
5. Yao, X., Gao, S., and Yan, N. (2024). Structural biology of voltage-gated calcium channels. Channels (Austin) *18*, 2290807. 10.1080/19336950.2023.2290807.
6. Inui, M., Saito, A., and Fleischer, S. (1987). Purification of the ryanodine receptor and identity with feet structures of junctional terminal cisternae of sarcoplasmic reticulum from fast skeletal muscle. J Biol Chem *262*, 1740-1747.
7. Lai, F.A., Erickson, H.P., Rousseau, E., Liu, Q.Y., and Meissner, G. (1988). Purification and reconstitution of the calcium release channel from skeletal muscle. Nature *331*, 315-319. 10.1038/331315a0.
8. Takeshima, H., Nishimura, S., Matsumoto, T., Ishida, H., Kangawa, K., Minamino, N., Matsuo, H., Ueda, M., Hanaoka, M., Hirose, T., and et al. (1989). Primary structure and expression from complementary DNA of skeletal muscle ryanodine receptor. Nature *339*, 439-445. 10.1038/339439a0.
9. Rios, E., and Brum, G. (1987). Involvement of dihydropyridine receptors in excitation-contraction coupling in skeletal muscle. Nature *325*, 717-720. 10.1038/325717a0.
10. Block, B.A., Imagawa, T., Campbell, K.P., and Franzini-Armstrong, C. (1988). Structural evidence for direct interaction between the molecular components of the transverse tubule/sarcoplasmic reticulum junction in skeletal muscle. J Cell Biol *107*, 2587-2600. 10.1083/jcb.107.6.2587.
11. Perni, S., Lavorato, M., and Beam, K.G. (2017). De novo reconstitution reveals the proteins required for skeletal muscle voltage-induced Ca(2+) release. Proc Natl Acad Sci U S A *114*, 13822-13827. 10.1073/pnas.1716461115.
12. Norris, N., Joseph, S., Aditya, S., Karunasekara, Y., Board, P., Dulhunty, A., Oakley, A., and Casarotto, M. (2017). Structural and biophysical analyses of the skeletal dihydropyridine receptor β subunit β 1a reveal critical roles of domain interactions for stability. The Journal of biological chemistry *292*. 10.1074/jbc.M116.763896.
13. Cheng, W., Altafaj, X., Ronjat, M., and Coronado, R. (2005). Interaction between the dihydropyridine receptor Ca2+ channel beta-subunit and ryanodine receptor type 1 strengthens excitation-contraction coupling. Proc Natl Acad Sci U S A *102*, 19225-19230. 10.1073/pnas.0504334102.
14. Rebbeck, R.T., Karunasekara, Y., Gallant, E.M., Board, P.G., Beard, N.A., Casarotto, M.G., and Dulhunty, A.F. (2011). The beta(1a) subunit of the skeletal DHPR binds to skeletal RyR1 and activates the channel via its 35-residue C-terminal tail. Biophys J *100*, 922-930. 10.1016/j.bpj.2011.01.022.
15. Takeshima, H., Komazaki, S., Nishi, M., Iino, M., and Kangawa, K. (2000). Junctophilins: a novel family of junctional membrane complex proteins. Mol Cell *6*, 11-22. 10.1016/s1097-2765(00)00003-4.
16. Perni, S., and Beam, K. (2022). Junctophilins 1, 2, and 3 all support voltage-induced Ca2+ release despite considerable divergence. J Gen Physiol *154*. 10.1085/jgp.202113024.

Langtaosha (LTS) Preprint doi: https://doi.org/10.65215/LTSpreprints.2026.11.20.000396. This version posted November 21, 2026. The copyright holder for this preprint (which was not certified by peer review) is the author/funder. All Rights Reserved. No reuse allowed without permission.

17. Rossi, D., Scarcella, A.M., Liguori, E., Lorenzini, S., Pierantozzi, E., Kutchukian, C., Jacquemond, V., Messa, M., De Camilli, P., and Sorrentino, V. (2019). Molecular determinants of homo- and heteromeric interactions of Junctophilin-1 at triads in adult skeletal muscle fibers. Proceedings of the National Academy of Sciences *116*, 15716-15724. doi:10.1073/pnas.1820980116.
18. Golini, L., Chouabe, C., Berthier, C., Cusimano, V., Fornaro, M., Bonvallet, R., Formoso, L., Giacomello, E., Jacquemond, V., and Sorrentino, V. (2011). Junctophilin 1 and 2 proteins interact with the L-type Ca2+ channel dihydropyridine receptors (DHPRs) in skeletal muscle. J Biol Chem *286*, 43717-43725. 10.1074/jbc.M111.292755.
19. Phimister, A.J., Lango, J., Lee, E.H., Ernst-Russell, M.A., Takeshima, H., Ma, J., Allen, P.D., and Pessah, I.N. (2007). Conformation-dependent stability of junctophilin 1 (JP1) and ryanodine receptor type 1 (RyR1) channel complex is mediated by their hyper-reactive thiols. J Biol Chem *282*, 8667-8677. 10.1074/jbc.M609936200.
20. Yang, Z.F., Panwar, P., McFarlane, C.R., Tuinte, W.E., Campiglio, M., and Van Petegem, F. (2022). Structures of the junctophilin/voltage-gated calcium channel interface reveal hot spot for cardiomyopathy mutations. Proc Natl Acad Sci U S A *119*, e2120416119. 10.1073/pnas.2120416119.
21. Horstick, E.J., Linsley, J.W., Dowling, J.J., Hauser, M.A., McDonald, K.K., Ashley-Koch, A., Saint-Amant, L., Satish, A., Cui, W.W., Zhou, W., et al. (2013). Stac3 is a component of the excitation-contraction coupling machinery and mutated in Native American myopathy. Nat Commun *4*, 1952. 10.1038/ncomms2952.
22. Nelson, B.R., Wu, F., Liu, Y., Anderson, D.M., McAnally, J., Lin, W., Cannon, S.C., Bassel-Duby, R., and Olson, E.N. (2013). Skeletal muscle-specific T-tubule protein STAC3 mediates voltage-induced Ca2+ release and contractility. Proc Natl Acad Sci U S A *110*, 11881-11886. 10.1073/pnas.1310571110.
23. Polster, A., Perni, S., Bichraoui, H., and Beam, K.G. (2015). Stac adaptor proteins regulate trafficking and function of muscle and neuronal L-type Ca²⁺ channels. Proceedings of the National Academy of Sciences *112*, 602-606. doi:10.1073/pnas.1423113112.
24. Wong King Yuen, S.M., Campiglio, M., Tung, C.C., Flucher, B.E., and Van Petegem, F. (2017). Structural insights into binding of STAC proteins to voltage-gated calcium channels. Proc Natl Acad Sci U S A *114*, E9520-e9528. 10.1073/pnas.1708852114.
25. Polster, A., Nelson, B.R., Papadopoulos, S., Olson, E.N., and Beam, K.G. (2018). Stac proteins associate with the critical domain for excitation-contraction coupling in the II-III loop of Ca(V)1.1. J Gen Physiol *150*, 613-624. 10.1085/jgp.201711917.
26. Campiglio, M., Costé de Bagneaux, P., Ortner, N.J., Tuluc, P., Van Petegem, F., and Flucher, B.E. (2018). STAC proteins associate to the IQ domain of Ca(V)1.2 and inhibit calcium-dependent inactivation. Proc Natl Acad Sci U S A *115*, 1376-1381. 10.1073/pnas.1715997115.
27. Radermacher, M., Wagenknecht, T., Grassucci, R., Frank, J., Inui, M., Chadwick, C., and Fleischer, S. (1992). Cryo-EM of the native structure of the calcium release channel/ryanodine receptor from sarcoplasmic reticulum. Biophys J *61*, 936-940. 10.1016/s0006-3495(92)81900-8.
28. Yan, Z., Bai, X., Yan, C., Wu, J., Li, Z., Xie, T., Peng, W., Yin, C., Li, X., Scheres, S.H.W., et al. (2015). Structure of the rabbit ryanodine receptor RyR1 at near-atomic resolution. Nature *517*, 50-55. 10.1038/nature14063.
29. Zalk, R., Clarke, O.B., des Georges, A., Grassucci, R.A., Reiken, S., Mancia, F., Hendrickson, W.A., Frank, J., and Marks, A.R. (2015). Structure of a mammalian ryanodine receptor. Nature *517*, 44-49. 10.1038/nature13950.
30. Wu, J., Yan, Z., Li, Z., Yan, C., Lu, S., Dong, M., and Yan, N. (2015). Structure of the voltage-gated calcium channel Cav1.1 complex. Science *350*, aad2395. 10.1126/science.aad2395.
31. Wu, J., Yan, Z., Li, Z., Qian, X., Lu, S., Dong, M., Zhou, Q., and Yan, N. (2016). Structure of the voltage-gated calcium channel Ca(v)1.1 at 3.6 Å resolution. Nature *537*, 191-196. 10.1038/nature19321.

Langtaosha (LTS) Preprint doi: https://doi.org/10.65215/LTSpreprints.2026.11.20.000396. This version posted November 21, 2026. The copyright holder for this preprint (which was not certified by peer review) is the author/funder. All Rights Reserved. No reuse allowed without permission.

32. Baumeister, W. (2022). Cryo-electron tomography: The power of seeing the whole picture. Biochem Biophys Res Commun *633*, 26-28. 10.1016/j.bbrc.2022.08.078.
33. Villa, E., Schaffer, M., Plitzko, J.M., and Baumeister, W. (2013). Opening windows into the cell: focused-ion-beam milling for cryo-electron tomography. Curr Opin Struct Biol *23*, 771-777. 10.1016/j.sbi.2013.08.006.
34. Xu, J., Liao, C., Yin, C.C., Li, G., Zhu, Y., and Sun, F. (2024). In situ structural insights into the excitation-contraction coupling mechanism of skeletal muscle. Sci Adv *10*, eadl1126. 10.1126/sciadv.adl1126.
35. Bai, X.C., Yan, Z., Wu, J., Li, Z., and Yan, N. (2016). The Central domain of RyR1 is the transducer for long-range allosteric gating of channel opening. Cell Res *26*, 995-1006. 10.1038/cr.2016.89.
36. Peng, W., Shen, H., Wu, J., Guo, W., Pan, X., Wang, R., Chen, S.R., and Yan, N. (2016). Structural basis for the gating mechanism of the type 2 ryanodine receptor RyR2. Science *354*. 10.1126/science.aah5324.
37. Chi, X., Gong, D., Ren, K., Zhou, G., Huang, G., Lei, J., Zhou, Q., and Yan, N. (2019). Molecular basis for allosteric regulation of the type 2 ryanodine receptor channel gating by key modulators. Proc Natl Acad Sci U S A *116*, 25575-25582. 10.1073/pnas.1914451116.
38. Gong, D., Chi, X., Wei, J., Zhou, G., Huang, G., Zhang, L., Wang, R., Lei, J., Chen, S.R.W., and Yan, N. (2019). Modulation of cardiac ryanodine receptor 2 by calmodulin. Nature *572*, 347-351. 10.1038/s41586-019-1377-y.
39. Pasut, A., Jones, A.E., and Rudnicki, M.A. (2013). Isolation and culture of individual myofibers and their satellite cells from adult skeletal muscle. J Vis Exp, e50074. 10.3791/50074.